J. Am. Soc. Mass Spectrom. (2019) 30:946–955
DOI: 10.1007/s13361-018-2094-8

FOCUS: ION MOBILITY SPECTROMETRY (IMS): RESEARCH ARTICLE

Effects of Individual Ion Energies on Charge Measurements in Fourier Transform Charge Detection Mass Spectrometry (FT-CDMS)

Andrew G. Elliott, Conner C. Harper, Haw-Wei Lin, Evan R. Williams

Department of Chemistry, University of California, Berkeley, CA 94720-1460, USA

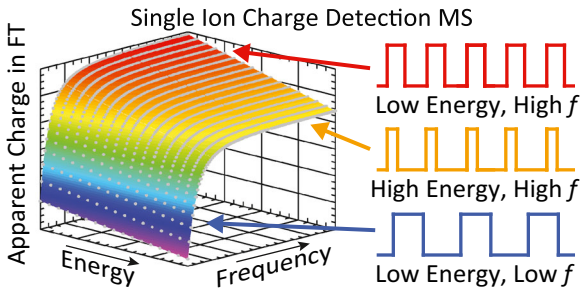

Abstract. A method to correct for the effect of ion energy on charge measurements of individual ions trapped and weighed with charge detection mass spectrometry (CDMS) is demonstrated. Ions with different energies induce different signal patterns inside an electrostatic ion trap. The sum of the amplitudes of the fundamental and second harmonic frequencies in the Fourier transform of the induced signal, which has been used to obtain the ion charge, depends on both ion energy and charge. The amplitudes of the fundamental frequencies of ions increase over time as ions lose energy by collisions with background gas and solvent loss from larger ions. Model ion signals are simulated with the same time-domain amplitude at different energies and frequencies and the resulting fundamental frequency amplitudes are used to normalize real ion signals for energy and frequency effects. The fundamental frequency amplitude decreases dramatically below 20 kHz and increases by ~ 17% from the highest energy to lowest energy that is stable with a given trap potential at all frequencies. Normalizing the fundamental frequency amplitude with the modeled amplitudes removes the systematic changes in the charge measurement of polyethylene glycol (PEG) and other ions and makes it possible to signal average the amplitude over long times, which reduces the charge uncertainty to 0.04% for a PEG ion for a 500-ms measurement. This method improves charge measurement accuracy and uncertainty, which are important for high-accuracy mass measurement with CDMS.

Keywords: Charge detection mass spectrometry, CDMS, Harmonics, Fourier transform, Ion energy, Ion charge

Received: 15 August 2018/Revised: 15 October 2018/Accepted: 15 October 2018/Published Online: 14 November 2018

Introduction

Electrospray ionization (ESI) can transfer large molecules and molecular complexes into the gas phase as multiply charged ions for their identification or structural analysis with mass spectrometry (MS). Masses of ions can be determined from the spacings between peaks in a charge-state distribution produced by molecules or complexes with the same mass or from the isotopic spacing of a single charge state, with all information obtained from ensemble measurements of many different ions. Heterogeneity in the masses of ions, both intrinsic to the analyte and due to salt and solvent adduction, can lead to broad, unresolved peaks which obscure the charge-state separation necessary for mass measurement when isotopic or adduct resolution is not possible [1]. Charges and masses have been measured for highly purified virus capsids up to ~ 18 MDa, but the upper mass limit is significantly lower for more heterogeneous samples, such as native viruses and synthetic polymers [2–4]. The issue of heterogeneity can be eliminated if the mass of each ion is determined individually, such as has been demonstrated in Fourier transform ion cyclotron resonance (FT-ICR) [5–7] and quadrupole ion trap (QIT) mass spectrometry [8–15]. Although accurate mass measurements can be made with these techniques, the long measurement time

Electronic supplementary material The online version of this article (https://doi.org/10.1007/s13361-018-2094-8) contains supplementary material, which is available to authorized users.

Correspondence to: Evan Williams; *e-mail:* erw@berkeley.edu

for each ion makes them impractical to use for analyzing complex samples.

Charge detection mass spectrometry (CDMS) is an alternative method for single ion MS that is faster than the FT-ICR and QIT techniques. In CDMS, single ions induce a charge pulse as they pass through a conductive detection tube. The charge of the ion is proportional to the amplitude of the charge pulse, and the *m*/*z* of the ion is proportional to its velocity, which is obtained from the duration of the charge pulse. The simplest implementation of CDMS, in which an ion passes once through a single detector, has been used to study a variety of different samples [16–25]. A single tube CDMS measurement is fast, but has the disadvantage of high uncertainty (> 75 *e*) in the charge measurement for each individual ion. Because the ion detection is nondestructive, the signal from an ion can be averaged from multiple measurements in order to reduce uncertainty in the charge measurement. Techniques involving electrostatic ion traps [26–29], arrays of aligned detector tubes [30–32], and a combined ion trap and array detector [33] have all been implemented to repetitively weigh an individual ion. However, most recent developments have been based on the single detector ion trap design first demonstrated by Benner, in which ions were trapped for up to 450 passes through the detector tube resulting in a charge uncertainty of 2.3 *e* [26]. Dugourd and coworkers have used this design to investigate the photodissociation of polyethylene glycol (PEG) and DNA ions [27, 34–36]. Jarrold and coworkers also used the single tube ion trap to develop a Fourier transform CDMS (FT-CDMS) technique in which the ion *m*/*z* is obtained from the oscillation frequency and the charge is obtained from the amplitude of the oscillation frequency and second harmonic frequency [28, 37]. An important feature of FT-CDMS is a low detection limit (~ 6 *e*), enabling the measurement of small, less highly charged proteins, such as ubiquitin and cytochrome *c* and large protein complexes including pyruvate kinase and numerous different virus particles [38–40]. They have also demonstrated an uncertainty in the charge measurement of 0.196 *e* rmsd, which was obtained with cryogenically cooled detector electronics and extended ion trapping times up to 3 s [37, 41].

Extending the trapping period reduces the uncertainty in the charge measurement caused by random noise, but other sources of uncertainty also affect the mass measurement. The oscillation frequency of an ion trapped for CDMS can change significantly while it oscillates inside the trap [42–44]. These frequency shifts can be caused not only by changes in the ion *m*/*z* through discrete fragmentation events and gradual mass loss due to solvent evaporation, but also by changes in the ion energy after collisions with the background gas. The relationship between energy and frequency leads to uncertainty in the *m*/*z* measurement for ions with different energies. Ions entering the trap with a wide range of energies or changing energy inside the device can obfuscate mass measurements. Energy filtering before the ion trap decreases the overall spread of ion energies that reaches the trap. This improves the uncertainty in the *m*/*z* obtained only from an initial frequency measurement, but not at later times when the energy and frequency of an ion changes inside the trap. High-resolution energy filtering can also reduce the rate at which ions enter the trap for dilute solutions for which few ions are formed, diminishing the throughput of the mass measurement.

Instead of using an energy filter, the ion energy can be measured dynamically while the ion is trapped by measuring the turning time ratio (TTR), the ratio of the time the ion takes to turn around in the trapping electrode to the time the ion takes to travel through the detector electrode [43]. The TTR is related to the duty cycle or fraction of each cycle through the trap an ion spends in the detector tube. With less energy, ions turn around faster in the field region but take longer to transit the detector tube in the field free region, leading to a higher duty cycle and higher oscillation frequency. Ion energies can also be measured using the ratio between the amplitudes of the first and second harmonics in the FT spectrum [45]. This ratio is highly dependent on the ion energy because the entire pattern of harmonic amplitudes changes when the duty cycle and thus the pattern of the periodic waveform induced by an ion changes. Thus, two ions with the same charge state and *m*/*z* with different energies will have different TTRs and different amplitudes at their fundamental frequencies, resulting in uncertainty in the charge measurement. With these in situ energy measurement techniques, CDMS can be used for tandem MS [43] and ion mobility measurements of single ions [43–45].

Here, we demonstrate a method to normalize FT-CDMS charge measurements for ion energy effects using the energy of each ion in situ during the mass measurement. The amplitude of the fundamental frequency in the FT of a real ion signal is scaled by the fundamental frequency amplitude of a model ion signal simulated at a range of frequencies and TTR values with a constant time-domain amplitude. Without the normalization, energy loss during the trapping period results in a systematic measurement error where the amplitude of the fundamental frequency increases steadily while each ion is trapped. The normalization essentially eliminates the slope in the measured amplitude over time for all ions. For highly charged ions that lose a large amount of energy, removing this systematic error in the charge measurement makes it possible to signal average the charge measurement over long times, reducing the uncertainty by up to two orders of magnitude.

Experimental

PEG with a nominal molecular weight of 4 MDa and bovine serum albumin (BSA) were obtained from Sigma-Aldrich (St. Louis, MO, USA) and were used without further purification. PEG was prepared at a concentration of 120 nM in 50:50 water-methanol and BSA was prepared at 10 μM in 50:50 water-methanol with 3% (*v*/*v*) acetic acid.

Experiments were performed using a home-built charge detection mass spectrometer (Figure 1) that is described in detail elsewhere [43]. Briefly, ions are formed by nanoelectrospray ionization using borosilicate capillaries pulled to tips with an inner diameter of ~ 1.5 μm. Ions enter the instrument through a modified Z-Spray source (Waters, Milford, MA, USA) and are transferred to the trap region by

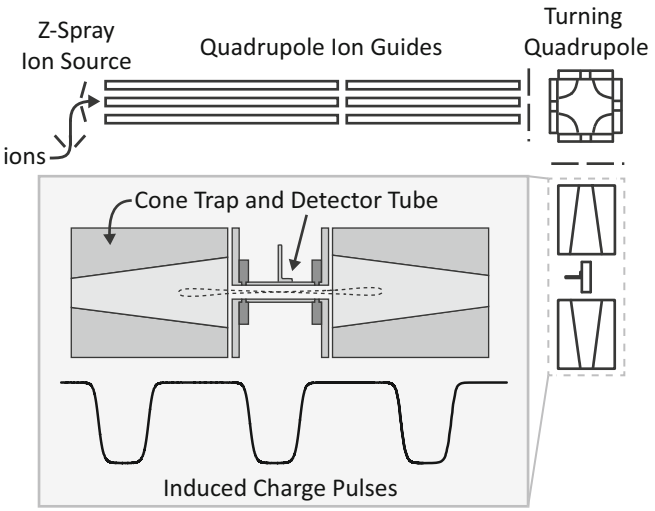

Figure 1. Overview of the instrument used in these experiments. The highlighted section of the diagram shows the detector tube and ion trap in detail, as well as an example trajectory for a trapped ion and the corresponding induced charge pulses. The shorter, negative, part of the waveform corresponds to the pulse induced by an ion

a pair of RF-only quadrupole ion guides and an energy selective electrostatic turning quadrupole (Ardara Technologies, Ardara, PA, USA). The electrostatic cone trap is in a differentially pumped chamber at a pressure of approximately 4×10^{-9} Torr. A detector, which consists of a single stainless steel tube that is 28.2 mm long and has an inner diameter of 7.1 mm, is located between the electrodes of the trap.

When an ion passes through the detector tube, it induces a charge pulse on the tube. The charge pulse is amplified by a CoolFET charge-sensitive preamplifier, linear voltage amplifier, and shaping amplifier (Amptek, Bedford, MA, USA). Data is recorded on two detection channels, one using the output from the linear amplifier and the other using the output of the shaping amplifier. The shaping amplifier produces a pair of peaks at the leading and trailing ends of the charge pulse. Ions with >300 charges can be detected above the noise in the time-domain signal on a single pass through the detector tube using the shaped signal. Thus, for high-charge ions, such as those formed from 4 MDa PEG, the shaped detection channel is used to control the operation of the ion trap. The peak produced by an ion entering the detector rises above a specified level, triggering the raising of the potential of the front electrode to match the constant potential of the back electrode for a specified time (500 ms in these experiments). For low-charge ions such as smaller proteins that are not sufficiently charged to be detected on a single pass, a random trapping scheme where the trap is opened and closed at regular intervals is used. In this scheme, the front electrode potential is held at 0 V for 1 ms then raised to match the constant potential of the back electrode for the specified trapping time (500 ms here), then lowered again to 0 V to allow the trapped ion to leave and restart the measurement cycle.

The time-domain signals generated by a trapped, oscillating ion are analyzed offline with LabVIEW programs described in detail previously [33, 44]. Trapped high-charge ions are identified using a program that finds peaks of consistent size and spacing in the shaped detection channel that persist for at least 5 ms. Trapped low-charge ions are identified by finding signals that last for at least 85 ms using a program that performs a short-time Fourier transform (STFT) routine and records the fundamental frequency and amplitude of the fundamental and a specified set of harmonics for each segment. The shaped signal has a better signal-to-noise (S/N) than the unshaped channel for ion detection and is therefore used to determine whether an ion is trapped. However, the shaping amplifier distorts the pattern of harmonic frequency amplitudes, so the unshaped signal is used for all analysis of the amplitudes of the fundamental and harmonic frequencies of ions. The segment length used in the STFT is adjusted depending on the sample. The segment length is chosen to optimize the balance between the signal-to-noise ratio improvement provided by a longer segment with the amplitude dampening caused by the ion frequency shifting during that time. For the 4 MDa PEG sample, the segment length is set to 5 ms, and for BSA, the segment length is set to 25 ms.

Results and Discussion

Charge Measurement of Single Ions

In CDMS, trapped ions produce periodic signals from which independent measures of m/z, charge, and hence mass can be obtained. Uncertainty in the m/z and charge measurements can be reduced with longer trapping times. The frequency of the ion oscillation is obtained from a Fourier transform (FT) of the time-domain signal induced by an ion. The oscillation frequency is related to the ion m/z and ion energy, and the amplitudes of the fundamental and harmonic frequencies are related to the ion charge and ion energy. The ion energy decreases during the time that it is trapped due to collisions with the background gas and, for some ions, mass loss owing either to solvent evaporation or fragmentation [42–44]. Energy loss due to collisions and solvent evaporation leads to an increase in the oscillation frequency. When the ion has less energy, it spends more time transiting through the detection tube owing to the lower velocity in this field-free region but turns around faster inside the trapping electrodes [43]. Thus, the ratio between the turn-around time and tube transit time or turning time ratio (TTR) decreases as the ion energy decreases, which causes the oscillation frequency to increase. Because the pattern of amplitudes at the fundamental frequency and higher harmonic frequencies depends on the ion energy, a FT spectrum of the induced signal changes over time as well [45].

The effect of changes in ion energy on the signal pattern produced by a polyethylene glycol (PEG) ion with 2496 ± 1 charges trapped for 500 ms is illustrated in Figure 2a, b. The oscillation frequency of the ion increases from 19.3 kHz between 5 and 10 ms (blue trace, Figure 2a, b) to 21.7 kHz between 495 and 500 ms (orange trace, Figure 2a, b). At these two times, the TTR measured from the shaped channel time-domain signal (Figure 2a) decreases from 2.31 to 1.85 (see

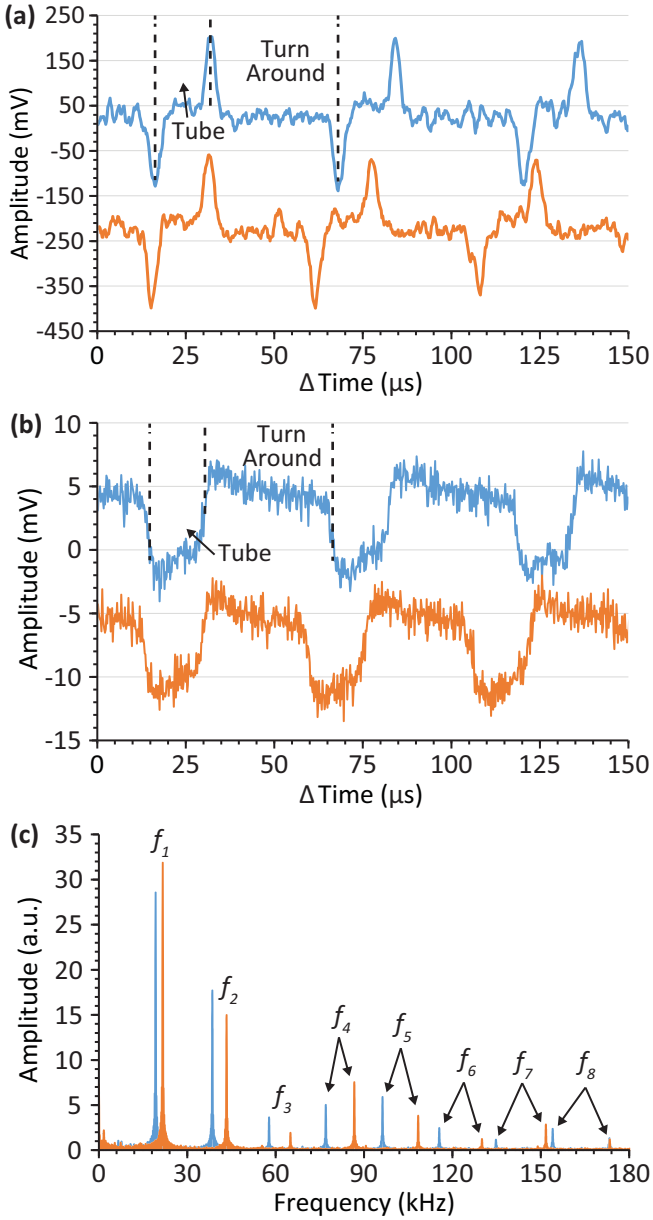

Figure 2. (**a**) Shaped channel time-domain signal and (**b**) unshaped channel time-domain signal for PEG transient starting at different times (blue, 5.12 ms into transient; orange, 495.08 ms into transient). (**c**) FTs of 5 ms segments of data starting at 5 ms (blue) and 495 ms (orange)

Supporting Information). The unshaped signal (Figure 2b) resembles a rectangular wave pulse train with a negative pulse while the ion is in the tube and positive pulse while the ion is turning around. The duty cycle, the fraction of the waveform with a negative pulse, increases from 30.2 to 35.1%, corresponding to the change in TTR. In the FT spectrum of the unshaped signal, the amplitude of the fundamental frequency increases by ~11% between these two time periods (Figure 2c). The relative amplitudes of the harmonic frequencies change as well, with the fourth and seventh harmonics increasing, and the second, third, fifth, sixth, and eighth harmonics decreasing between the two time periods. Higher harmonic frequencies beyond the eighth harmonic also change in amplitude, each with their own pattern. Although the fundamental and harmonic amplitudes change with time, the amplitude of the signal pulse in the time domain does not change. This clearly demonstrates that the change in the amplitude of the fundamental and harmonic frequencies is due to changing ion energy and not ion charge, which remains constant throughout the measurement. This illustrates the challenge of determining the ion charge from the amplitudes of the fundamental frequency and just one or a few harmonic frequencies in the FT spectrum as they change over time.

The amplitude of the periodic time-domain signal induced by an ion is proportional to the ion charge. For an ideal periodic signal, the time-domain amplitude can be obtained from the sum of the amplitudes of the fundamental frequency and each of the harmonic frequencies in the FT spectrum. Signal-to-noise ratios and sampling rate limitations make including many higher order harmonic frequencies in this sum challenging for real CDMS ion signals, especially for low-charge ions. As a result, the charge of the ion is instead typically taken to be proportional to the amplitude of the fundamental or the sum of the fundamental and second harmonic frequency, the two most intense frequencies [37]. However, this proportionality is only exact when comparing signal patterns that have the same duty cycle and therefore produce the same pattern of harmonics. Because the pattern of harmonic frequencies changes as the ion energy decreases with time, the proportionality between charge and the amplitudes of a single or set of harmonic frequencies also changes. Determining the charge from FT amplitudes without considering the ion energy during the time segment in each transform can thus lead to errors in charge measurements.

To illustrate the errors in determining ion charge that can occur if the ion energy is not taken into account, the apparent charge obtained from the amplitude of the fundamental frequency of the ion from Figure 2 is shown as a function of time in Figure 3 (blue triangles). The amplitude monotonically increases over the entire 500 ms trapping time. Calibrating the charge measurement at the initial ion energy, the slope of these data suggests that the ion gains one charge every ~1.8 ms (~280 charges over 500 ms) during this trap time. However, the time-domain signal shows that no change in charge occurs for this ion. This discrepancy is a clear indication of a systematic measurement error that occurs because the ion energy decreases over time. This error increases significantly over time, so the apparent charge obtained from the average amplitude of segments in the first 100 ms (2525 *e*) is smaller than apparent charge using the average amplitude of all segments in the entire trapping time (2647 *e*). Signal averaging for longer times only increases the uncertainty and changes the charge obtained in these measurements because the uncertainty is predominantly caused by a systematic error rather than random noise.

The systematic error is mitigated somewhat by summing the fundamental and second harmonic frequencies (Figure 3, black points). The summed amplitude increases in the first ~200 ms before reaching a maximum and decreases with a smaller slope over the final ~200 ms. Using local regression to fit the

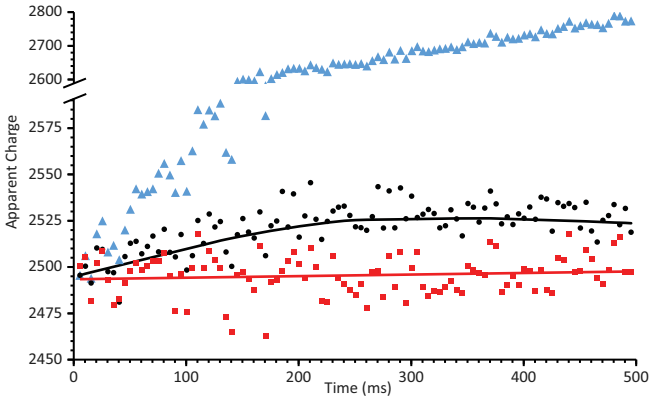

Figure 3. Comparison of the time evolution of the apparent charge of the PEG ion shown in Fig. 2 determined from the fundamental frequency amplitude (blue triangles), sum of the fundamental and second harmonic frequency amplitudes (black circles and black line showing local regression) and using the fundamental amplitude charge normalization (red squares and red line showing linear regression). For the normalized data, the charge response of the detector was calibrated with protein ions in resolved charge states. For the non-normalized data, the apparent charge was determined by assigning the initial amplitude measurement to the ion charge (2496 *e*) and scaling the remaining points accordingly

nonlinear change in amplitude over time, the summed amplitude varies by ~ 1.2% from its maximum to its minimum, corresponding to a ~ 1.2% or ~ 31 *e* change in charge based on the charge calibration at the initial ion energy. The change in amplitude for the summed amplitudes is smaller than for the fundamental frequency alone because the second harmonic decreases in amplitude over the range of TTRs the ion has while trapped which partially compensates for the increase in amplitude of the fundamental frequency that occurs with time. However, there is still a systematic measurement error because the amplitude of the second harmonic frequency changes at a different rate than the amplitude of the fundamental frequency. For high-charge ions, such as this PEG ion, the amplitudes of additional higher order harmonics are above the noise. Each harmonic frequency changes in amplitude with a different trend as the TTR changes over time (see Supporting Information). Some combination of different harmonics may further reduce the systematic measurement error, which is the primary factor in the overall uncertainty in the charge measurement made using the amplitude of the fundamental frequency or the sum of the amplitudes of the fundamental and second harmonic frequencies for this ion. However, the S/N is lower for these higher frequency harmonics, so adding their amplitudes to the fundamental amplitude increases the uncertainty caused by random noise. Between the reduced systematic error and increased random error, adding additional harmonics can either increase or decrease the overall uncertainty, depending on the charge of the ion and the rate at which the ion energy changes with time.

Changes in the ion energy and thereby TTR and fundamental frequency amplitude also occur over time for much smaller protein ions. Measuring the resulting systematic change in amplitude for these protein ions can be challenging because their slower energy loss reduces the relative change in the fundamental frequency amplitude over the trapping time. That relative change in charge also corresponds to a smaller absolute change in charge because the protein ions have fewer charges. Thus, for a single ion, the systematic amplitude change can be obscured by random noise. However, the systematic amplitude change can still be observed by combining data from many single ion measurements. Figure 4a shows the most common fundamental frequency amplitude measured for a 48+ bovine serum albumin (BSA) ion at different times in the 500 ms trapping period obtained from a Gaussian fit of the amplitude distribution at each time for a sample of 246 ions. The best fit line corresponds to a ~ 1% or ~ 0.5 *e* change in charge over 500 ms. Although the increase in amplitude with longer trap times is small, the *p* value for the slope is 1×10^{-4}, indicating that it is statistically significant. The increase in amplitude cannot be caused by a change in the charge state of the ions. This would result in a sudden change in oscillation frequency of at least ~ 600 Hz due to the change in the ion *m*/*z*, and this was not observed for any of these ions. Instead, the increase in

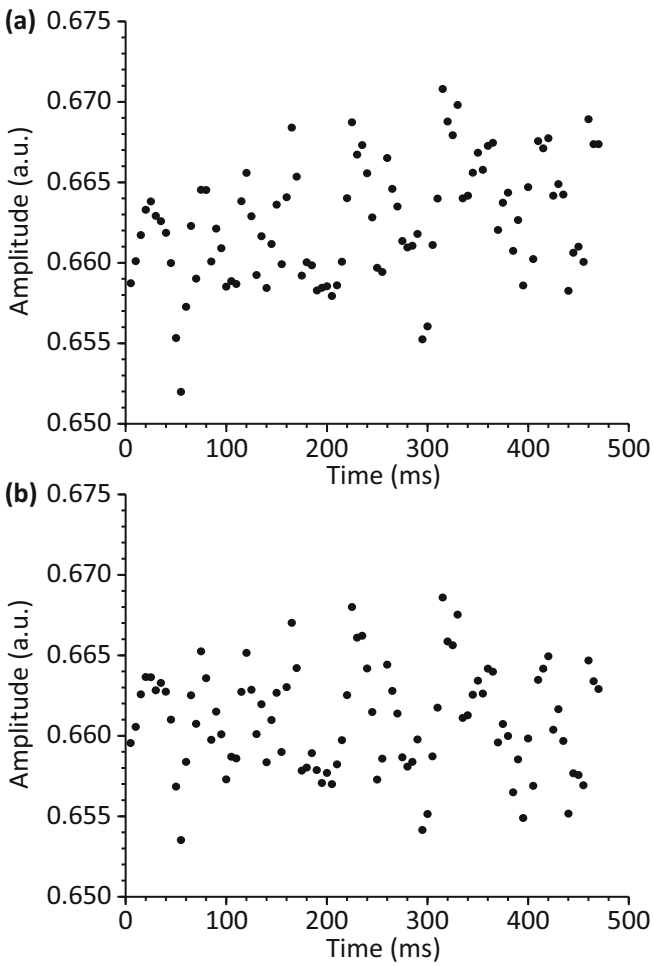

Figure 4. (**a**) Most probable fundamental frequency amplitude and (**b**) most probable normalized fundamental frequency amplitude for a sample of 246 48+ BSA ions at different times throughout the transient

amplitude occurs because the ions slowly lose energy, ~ 4.2 eV per charge, over the 500 ms trapping time. This change in energy results in a longer duty cycle (increasing from 35.7 to 36.3%) and a lower TTR (decreasing from 1.80 to 1.76). The pattern of the harmonic frequency amplitudes changes accordingly, with a larger proportion of the time-domain amplitude partitioned into the fundamental frequency. Because the BSA ions lose less energy than the much larger PEG ion shown previously, the systematic change in amplitude due to energy change is much smaller. The distribution of amplitudes caused by random noise variance is only slightly shifted by the systematic amplitude change. As a result, the overall distribution of BSA amplitudes is still nearly Gaussian, and the uncertainty in the mean amplitude still decreases over the entire 500 ms trapping time. At longer trapping times, however, the systematic effect of the changing harmonic amplitudes limits the improvement in the uncertainty if the ion energy and TTR are not taken into account.

Normalizing Fundamental Frequency Amplitudes for Energy

The amplitude of a fundamental frequency in the FT of a trapped ion signal depends on the frequency, TTR, and charge of the ion, but is linearly proportional to charge at any given combination of frequency and TTR. The effects of frequency and TTR on the charge measurement can be essentially eliminated by rescaling each amplitude measurement to normalize for these factors. The general scheme for this fundamental amplitude to charge normalization (FACN) is as follows. First, simulated ion signals are created with the same amplitude in the time domain for a wide range of different TTRs and frequencies. Each simulated signal is transformed to obtain the resulting amplitude of the fundamental frequency in the FT. All differences in the fundamental frequency amplitudes are then the result of varying amplitudes of the harmonic frequencies and not the amplitude of the time-domain signal. The amplitude of the fundamental frequency of an ion is then divided by the amplitude of the fundamental frequency of the simulated signal that has the same frequency and TTR as the ion, to normalize for any differences in the amplitude caused by the different pattern of harmonic frequency amplitudes. This FACN approach to accounting for the effects of ion energy on the amplitude of the fundamental frequency has two advantages. First, the fundamental frequency is the best frequency to normalize because it has the highest S/N and correspondingly the least relative uncertainty caused by random noise of any harmonic frequency. Random noise introduced to the measurement by adding higher harmonics that have lower S/N than the fundamental frequency can lower the overall S/N even though the systematic error is reduced. Second, scaling based on measured TTR also normalizes the amplitude of the fundamental frequency for any effects of differences in the ion trajectory. Although TTR depends primarily on the ion energy, it is also affected by the ion trajectory. Ions with trajectories off the central axis of the trap turn around faster in the trapping electrode and have a slightly lower TTR than ions with the same energy on the trap axis [43]. This leads to slightly different TTRs and duty cycles for ions with the same energy because ions do not necessarily all follow the same trajectory. However, the pattern of harmonic amplitudes reflects the actual TTR and duty cycle measured for the ion, rather than the ion energy directly. After applying the resulting normalization factor, ion signals can be compared with the same proportionality between charge and peak amplitudes.

In order to determine these normalization factors, the ion signal was simulated at a series of frequencies and TTRs using a method that has been described previously [45]. Briefly, signals ranging from 5 to 95 kHz and 1.6 to 2.4 in TTR were generated with the same maximum amplitude at the midpoint of the charge pulse. SIMION simulations indicate that this is the most extreme range of TTRs for trapped ions in this cell geometry. The rise time and shape of the charge pulse were determined from Green's reciprocity theorem and simulations of the trap geometry in SIMION [46]. RC decay was then iteratively applied across each simulated signal using a time constant of 20 μs to match the waveforms produced by real ions [47]. A comparison between the simulated and real signals for ions at ~ 20 kHz with 2.15 TTR and ~ 61 kHz and 1.80 TTR are shown in Figure 5a, b, respectively. The signal for the real ion is averaged over 5 ms with a comb filter that uses the locations of peaks in the shaped detection channel as reference points to add the signal to itself, and then scaled to the same amplitude as the simulated signal. The signals closely match during the charge pulse (corresponding to the ion traveling through the detector), but there is a small deviation in the decay shortly after the end of the charge pulse, especially at lower frequencies. RC decay significantly affects the shape of the lower frequency signal so the amplitude corresponding to the ion traveling halfway through the tube is decreased and the waveform deviates more significantly from a rectangular pulse train. The RC decay also changes the proportionality between the charge and the amplitude at the start of the pulse because some of the charge decays during the long rise time of the pulse. RC decay while the ion is not in the detector tube also makes measuring that amplitude in the time domain more challenging.

Results from the simulated signals (gray points, Figure 6a) show the effect of both TTR and RC decay on the amplitude of the fundamental frequency of the ion signal. The amplitude of the fundamental frequency is lower for higher values of TTR, corresponding to lower duty cycles, at all frequencies. At a single frequency, the amplitude at a TTR of 1.6 is ~ 17% larger than the value at a TTR of 2.4. At a single TTR, the fundamental amplitude changes only slightly between 40 and 95 kHz, but drops off quickly below 20 kHz due to the effect of RC decay on the shape of the induced signal. As the charge pulse shifts from resembling a rectangular pulse train to something closer to a sawtooth wave at low frequency, more intensity in the FT spectrum shifts from the fundamental frequency to higher harmonic frequencies. To determine the scaling factor for actual ion signals with frequencies and TTRs between the simulated signals, the FT fundamental amplitudes from the

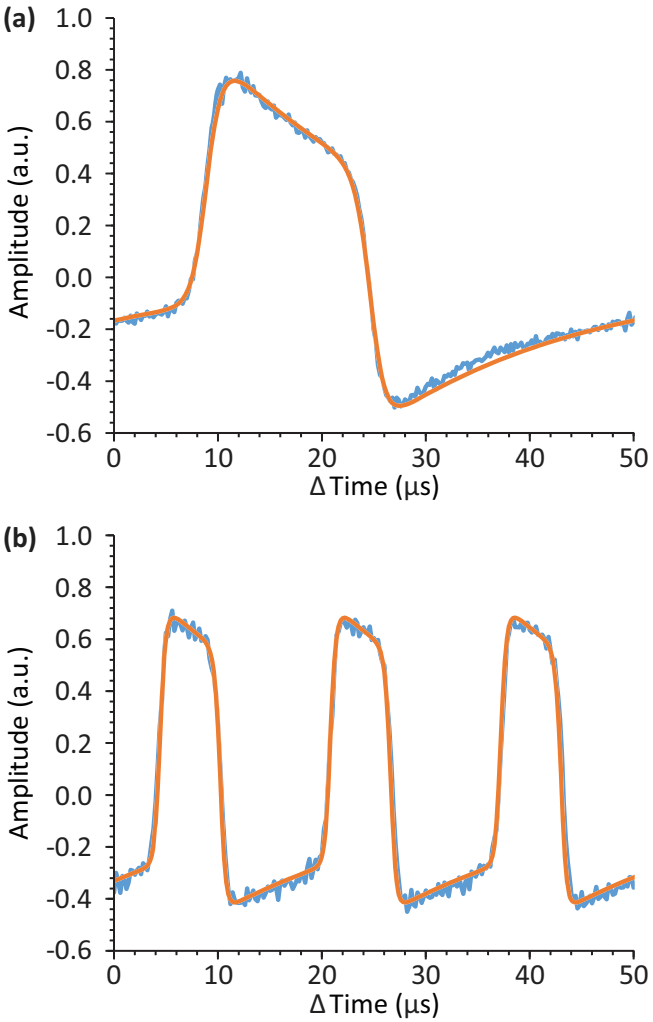

Figure 5. Comparison between real and simulated signals at (**a**) ~ 20 kHz and (**b**) ~ 60 kHz. Real signals are shown in blue and simulated signals are shown in orange

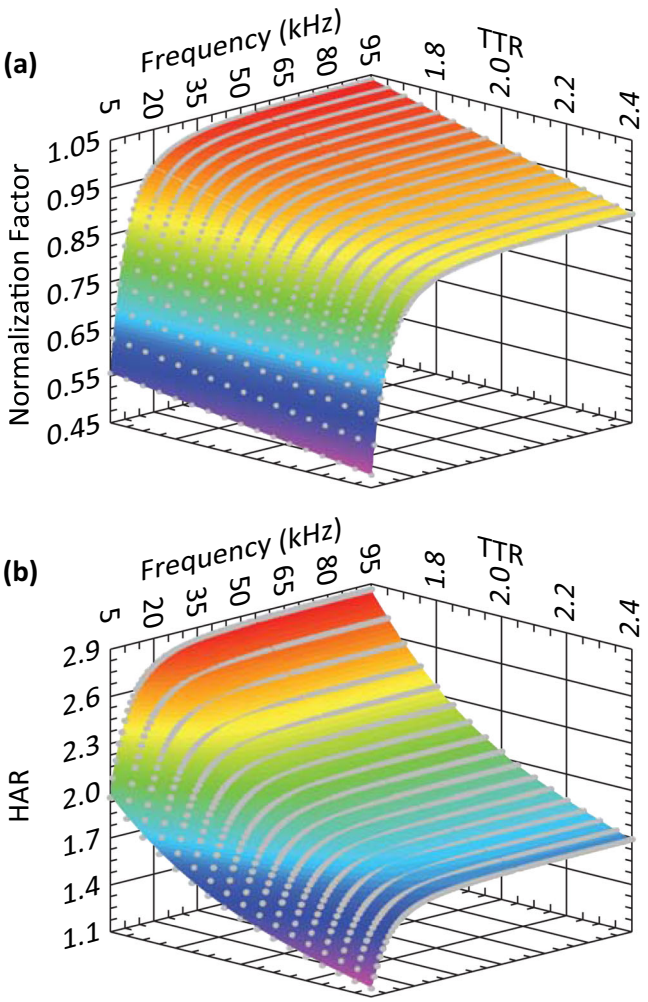

Figure 6. (**a**) Fundamental amplitude to charge normalization surface and (**b**) harmonic ratio surface determined from simulated model ion signals. The simulated points are shown in gray, and the surface fit to those points is shown in color

simulated signals were modeled with a function that is exponential in frequency and linear in TTR with a single cross term given by Eq. (1):

$$\text{Normalization factor} = a_1 e^{a_2 f} + a_3 TTR + a_4 TTR e^{a_2 f} + a_5 \quad (1)$$

which produces the colored surface shown in Figure 6a. To improve the fit to the simulated amplitudes, the data were divided in three groups, from 5 to 20 kHz, 20 to 50 kHz, and 50 to 95 kHz and each group was fit separately. The resulting sets of coefficients are provided in the Supporting Information. The exponential relationship between the scaling factor and frequency makes correctly scaling the amplitude at low frequency challenging. Because the scaling factors change rapidly in this regime, small errors in the modeled waveform can lead to larger uncertainty in the fundamental frequency amplitude and the resulting scaling factor. This could best be remedied by using higher ion energies in the trap resulting in higher fundamental frequencies or by increasing the RC time constant of detection system.

Measuring the TTR of each trapped ion accurately is important to effectively correct the amplitude measurement and hence the measure of the ion charge. A method to determine the TTR from the harmonic amplitude ratio (HAR) between the first and second harmonics has recently been demonstrated using ions that have a fundamental frequency of approximately 40 kHz [45]. Using the same simulations as above, the relationship between HAR and TTR can be determined at all frequencies (Figure 6b). Similarly to the fundamental amplitude, the HAR-TTR relationship changes only slightly above 40 kHz and changes significantly at lower frequencies. With this surface, the TTR can be determined for any ion that has detectable fundamental and second harmonic frequencies. This method is more generally applicable than the two methods that have previously been used to measure the TTR of an ion while it is trapped [43, 44]. For ions with more than ~ 300 charges, TTR can be measured from the time-domain signal after the square wave signal is passed through a shaping amplifier, which produces peaks that correspond to the ion entering and exiting the detector tube [43]. For ions with fewer charges, the TTR has

been determined from the oscillation frequency for ions with known m/z values [44]. This method requires that the ion is measured under instrument conditions where the relationship between the initial oscillation frequency and m/z is calibrated using the resolved charge state distribution of an ion with known mass. The HAR method is applicable to ions of any charge and unknown m/z. Thus, the TTR and the amplitude normalization factor can be determined for ions with a wider range of frequencies and charges than previously demonstrated.

Fundamental Amplitude to Charge Normalization for Individual Ions

Using the relationship between fundamental frequency amplitude, oscillation frequency and TTR, effects of changes in ion energy or trajectory on the charge measurement can be significantly reduced. The effect of the FACN method for the high-charge PEG ion is demonstrated in Figure 3 (red squares). For each 5 ms segment, the original fundamental amplitude was divided by a different normalization factor obtained from Eq. (1). The frequency and TTR of the ion during each segment were measured in the FT spectrum using the unshaped signal and time-domain signal using the shaped signal, respectively. The slope of the best fit line is ~ 60 times smaller than that for the non-normalized fundamental amplitude (Figure 3, blue triangles). The R^2 for the linear fit is 0.012 and the p value for the slope is 0.27. Using local regression to find a nonlinear change in the FACN amplitude, the maximum variation from the initial measurement is reduced by a factor of ~ 5 compared to the sum of the first and second harmonic frequency amplitudes. Because of the reduced dependence on TTR and frequency, the FACN amplitude can be accurately converted directly to a charge measurement. The standard deviation for the measured charge in each segment is 11 e, resulting in a charge uncertainty of 2.2 e after 125 ms and 1.1 e after the 500 ms trapping time. The charge uncertainty decreased by a factor of two after increasing the trapping time by a factor of four, following the expected dependence on the square root of the trapping time. Without the FACN, there is a lower limit to the charge uncertainty that can be obtained with increasing trapping time that is determined by the rate at which an ion loses energy. With no normalization, the charge uncertainty improves with longer trapping times until energy loss creates a large enough systematic change in amplitude that the overall distribution of amplitudes broadens significantly.

The FACN method is similarly effective for ions with any charge. Figure 4b shows the amplitudes that result from applying the appropriate normalization factors to the same sample of 48+ BSA ions shown in Figure 4a. Because these ions have too little charge to be directly observed in the time-domain signal, the TTR for each ion was determined from the measured frequency and the m/z assigned to the ion based on its charge state. After applying the FACN, the signal amplitude induced by the BSA ions does not change significantly over the course of the trapping time. The slope of a best fit line is -7.4×10^{-7}, which is opposite in sign and ~ 14 times smaller in magnitude than the slope of the un-normalized data. The p value for the slope is 0.77 which indicates that the time of the segment is not a significant factor in the measured amplitude. Because the amplitudes shown are from the entire sample of 48+ BSA ions, the variance in these data corresponds to an uncertainty in the average amplitude induced by a 48+ ion of 0.04 e, which is an uncertainty in the calibration. For individual ions in this charge state, the charge uncertainty of an ion measured for 500 ms is 0.58 e which is comparable to the charge uncertainty of 0.49 e reported by Jarrold and coworkers for ions trapped for ~ 400 ms [38]. The slightly lower charge uncertainty reported by Jarrold and coworkers is likely due to the lower temperature of their preamplifier (~ 125 K) compared to ~ 225 K in the instrument described here [41]. After correcting for differences in trapping time and temperature, the measurement uncertainty in both instruments is similar. The FACN does not result in a significant charge uncertainty improvement because the ions lose only a small amount of energy to collisions so failing to correct for TTR change introduces less error in the charge measurement for these smaller ions. The normalization becomes more important at longer trapping times, and for larger ions that lose energy more quickly.

The absolute charge uncertainty for individual BSA ions measured here is also less than it is for the PEG ion. Jarrold and coworkers have previously noted that the uncertainty in the charge measurement depends on the charge of the ion [37]. They attributed this to a combination of $1/f$ noise that increases the electrical noise for high m/z ions and a duty cycle effect that scales with charge. Here, applying the FACN significantly reduces the duty cycle effects of energy and trajectory, but the charge uncertainty for the PEG ion is still 1.9 times larger than that for the BSA ions. Approximately half of the difference in uncertainty can be attributed to $1/f$ noise. The baseline noise is ~ 30% higher at 20 kHz than at 65 kHz, and the FACN further increases the noise because the PEG ion is at higher TTR and lower frequency where the fundamental frequency amplitude is reduced. This frequency effect will tend to increase the noise for large ions which are often at high m/z and oscillate at lower frequency, but results in the same noise level for all ions at a given frequency and TTR. The remainder of the increased charge uncertainty is likely caused by duty cycle effects that the FACN does not completely account for. However, even with this small charge dependence for the absolute charge uncertainty, the relative charge uncertainty significantly improves so that it decreases with increasing charge. Without the FACN, the systematic change in amplitude caused by energy loss is the dominant source of charge uncertainty for high-charge ions. All ions with the same TTR change have the same relative change in amplitude, which creates a lower limit on the relative uncertainty in the charge measurement. For the PEG ion, the un-normalized fundamental frequency amplitude varies by ~ 11% from the beginning to the end of the transient. With the FACN, the relative charge uncertainty is just 0.04%. With such a small relative charge uncertainty, m/z uncertainty is the primary factor in the overall mass uncertainty even with an absolute charge uncertainty of 1.1 e.

Conclusions

Charge measurements in FT-CDMS can be improved by taking into account the effects of ion energy and oscillation frequency on the signal induced by an ion. The signal pattern or duty cycle depends on these factors, which in turn affects how the amplitude of the charge pulse in the time domain is distributed into the fundamental frequency and each of the harmonic frequencies in the frequency domain. Thus, determining the ion charge using only the fundamental frequency amplitude or the amplitudes of the fundamental and second harmonic frequencies leads to errors in the charge measurement. These errors can be significantly reduced with a correction method that uses the measured TTR and frequency to normalize the fundamental frequency amplitude for the effects of ion energy and detector electronics on the amplitude of signals in the frequency domain. The FACN method is especially important for large ions with high charge for which the change in amplitude is significantly larger than the random noise in the charge measurement. The fundamental frequency amplitude of a PEG ion with 2496 charges which gradually loses ~ 36 eV/charge over the 500 ms trapping time increases by 11% without the normalization and is essentially constant with the normalization. Because the normalized amplitude is constant, the charge measurement can be signal averaged over the entire trapping time, reducing the relative uncertainty in the charge to 0.04%.

Jarrold and coworkers have recently shown the dependence of the ion oscillation frequency on energy is significantly decreased in a trap that uses a harmonic potential [48]. The effect of energy on the fundamental frequency was reduced by an order of magnitude, leading to a factor of four improvement in the *m*/*z* resolution. The ion trap was also designed to obtain a duty cycle of 50% at the specified ion energy to eliminate the second harmonic and maximize the amplitude of the fundamental frequency to reduce the uncertainty in the charge measurement. However, with a detection tube of finite length, the duty cycle and the resulting charge measurement depend on the ion energy, even in a trap with harmonic potentials. For two ions with the same *m*/*z* and different energies in a harmonic trap, the lower energy ion will take longer to travel through the detector, and less time to turn around outside the detector. As a result, the ions have a different duty cycle and a different pattern of harmonic amplitudes, just as in the trap demonstrated here. Measuring the ion energy and using the FACN can remove these duty cycle effects. This approach has the added advantage that tracking how the ion energy changes over time also provides information about the ion cross section and makes MS/MS measurements possible [43–45]. Energy filtering to select a small slice of the ion population into the trap is also unnecessary with this approach. Accurate charge measurements can be made over a wide range of initial ion energies after measuring the ion energy in situ and normalizing the amplitude to remove duty cycle effects, establishing a universal charge calibration. Less energy filtering is advantageous for analyzing dilute samples from which few ions are formed, so all ions that can be trapped are actually measured. Measuring the ion energy and normalizing the fundamental frequency amplitude for that measured energy is thus an important way to reduce the influence of ion energy on the charge and mass measurement.

Acknowledgements

This material is based upon work supported by the National Science Foundation under CHE-1609866. The authors thank Professors Gert von Helden, Martin F. Jarrold, and David E. Clemmer for many helpful discussions and for their pioneering contributions to instrumentation and ion mobility spectrometry.

References

1. Lössl, P., Snijder, J., Heck, A.J.R.: Boundaries of mass resolution in native mass spectrometry. J. Am. Soc. Mass Spectrom. **25**, 906–917 (2014)
2. Snijder, J., Rose, R.J., Veesler, D., Johnson, J.E., Heck, A.J.: Studying 18 MDa virus assemblies with native mass spectrometry. Angew. Chem. Int. Ed. **52**, 4020–4023 (2013)
3. Weiss, V.U., Bereszczak, J.Z., Havlik, M., Kallinger, P., Gösler, I., Kumar, M., Blaas, D., Marchetti-Deschmann, M., Heck, A.J.R., Szymanski, W.W., Allmaier, G.: Analysis of a common cold virus and its subviral particles by gas-phase electrophoretic mobility molecular analysis and native mass spectrometry. Anal. Chem. **87**, 8709–8717 (2015)
4. Robb, D.B., Brown, J.M., Morris, M., Blades, M.W.: Method of atmospheric pressure charge stripping for electrospray ionization mass spectrometry and its application for the analysis of large poly(ethylene glycol)s. Anal. Chem. **86**, 9644–9652 (2014)
5. Smith, R.D., Cheng, X., Brace, J.E., Hofstadler, S.A., Anderson, G.A.: Trapping, detection and reaction of very large single molecular ions by mass spectrometry. Nature. **369**, 137–139 (1994)
6. Bruce, J.E., Cheng, X., Bakhtiar, R., Wu, Q., Hofstadler, S.A., Anderson, G.A., Smith, R.D.: Trapping, detection, and mass measurement of individual ions in a Fourier transform ion cyclotron resonance mass spectrometer. J. Am. Chem. Soc. **116**, 7839–7847 (1994)
7. Chen, R., Wu, Q., Mitchell, D.W., Hofstadler, S.A., Rockwood, A.L., Smith, R.D.: Direct charge number and molecular weight determination of large individual ions by electrospray ionization Fourier transform ion cyclotron resonance mass spectrometry. Anal. Chem. **66**, 3964–3969 (1994)
8. Wuerker, R.F., Shelton, H., Langmuir, R.V.: Electrodynamic containment of charged particles. J. Appl. Phys. **30**, 342–349 (1959)
9. Philip, M.A., Gelbard, F., Arnold, S.: An absolute method for aerosol particle mass and charge measurement. J. Colloid Interface Sci. **91**, 507–515 (1983)
10. Hars, G., Tass, Z.: Application of quadrupole ion trap for the accurate mass determination of submicron size charged particles. J. Appl. Phys. **77**, 4245–4250 (1995)
11. Schlemmer, S., Illemann, J., Wellert, S., Gerlich, D.: Nondestructive high-resolution and absolute mass determination of single charged particles in a three-dimensional quadrupole trap. J. Appl. Phys. **90**, 5410–5418 (2001)
12. Cai, Y., Peng, W.P., Kuo, S.J., Lee, Y.T., Chang, H.C.: Single-particle mass spectrometry of polystyrene microspheres and diamond nanocrystals. Anal. Chem. **74**, 232–238 (2002)
13. Nie, Z., Tzeng, Y., Chang, H., Chiu, C., Chang, C., Chang, C., Tao, M.: Microscopy-based mass measurement of a single whole virus in a cylindrical ion trap. Angew. Chem. Int. Ed. **45**, 8131–8134 (2006)
14. Bell, D.M., Howder, C.R., Johnson, R.C., Anderson, S.L.: Single CdSe/ZnS nanocrystals in an ion trap: charge and mass determination and photophysics evolution with changing mass, charge, and temperature. ACS Nano. **8**, 2387–2398 (2014)

15. Peng, W., Lin, H., Lin, H., Chu, M., Yu, A.L., Chang, H., Chen, C.: Charge-monitoring laser-induced acoustic desorption mass spectrometry for cell and microparticle mass distribution measurement. Angew. Chem. Int. Ed. **46**, 3865–3869 (2007)
16. Shelton, H., Hendricks, C.D., Wuerker, R.F.: Electrostatic acceleration of microparticles to hypervelocities. J. Appl. Phys. **31**, 1243–1246 (1960)
17. Hendricks Jr., C.D.: Charged droplet experiments. J. Colloid Sci. **17**, 249–259 (1962)
18. Keaton, P.W., Idzorek, G.C., Rowton Sr., L.J., Seagrave, J.D., Stradling, G.L., Bergeson, S.D., Collopy, M.T., Curling Jr., H.L., McColl, D.B., Smith, J.D.: A hypervelocity - microparticle - impacts laboratory with 100-km/s projectiles. Int. J. Impact Eng. **10**, 295–308 (1990)
19. Stradling, G.L., Idzorek, G.C., Shafer, B.P., Curling Jr., H.L., Collopy, M.T., Blossom, A.A.H., Fuerstenau, S.: Ultra-high velocity impacts: cratering studies of microscopic impacts from 3 km/s to 30 km/s. Int. J. Impact Eng. **14**, 719–727 (1993)
20. Fuerstenau, S.D., Benner, W.H.: Molecular weight determination of megadalton DNA electrospray ions using charge detection time-of-flight mass spectrometry. Rapid Commun. Mass Spectrom. **9**, 1528–1538 (1995)
21. Schultz, J.C., Hack, C.A., Benner, W.H.: Mass determination of megadalton-DNA electrospray ions using charge detection mass spectrometry. J. Am. Soc. Mass Spectrom. **9**, 305–313 (1998)
22. Fuerstenau, S.D., Benner, W.H., Thomas, J.J., Brugidou, C., Bothner, B., Siuzdak, G.: Mass spectrometry of an intact virus. Angew. Chem. Int. Ed. **40**, 542–544 (2001)
23. Doussineau, T., Kerleroux, M., Dagany, X., Clavier, C., Barbaire, M., Maurelli, J., Antoine, R., Dugourd, P.: Charging megadalton poly(ethylene oxide)s by electrospray ionization. A charge detection mass spectrometry study. Rapid Commun. Mass Spectrom. **25**, 617–623 (2011)
24. Doussineau, T., Désert, A., Lambert, O., Taveau, J., Lansalot, M., Dugourd, P., Bourgeat-Lami, E., Ravaine, S., Duguet, E., Antoine, R.: Charge detection mass spectrometry for the characterization of mass and surface area of composite nanoparticles. J. Phys. Chem. C. **119**, 10844–10849 (2015)
25. Doussineau, T., Mathevon, C., Altamura, L., Vendrely, C., Dugourd, P., Forge, V., Antoine, R.: Mass determination of entire amyloid fibrils by using mass spectrometry. Angew. Chem. Int. Ed. **55**, 2340–2344 (2016)
26. Benner, W.H.: A gated electrostatic ion trap to repetitiously measure the charge and *m/z* of large electrospray ions. Anal. Chem. **69**, 4162–4168 (1997)
27. Doussineau, T., Yu Bao, C., Clavier, C., Dagany, X., Kerleroux, M., Antoine, R., Dugourd, P.: Infrared multiphoton dissociation tandem charge detection-mass spectrometry of single megadalton electrosprayed ions. Rev. Sci. Instrum. **82**, 084104 (2011)
28. Contino, N.C., Jarrold, M.F.: Charge detection mass spectrometry for single ions with a limit of detection of 30 charges. Int. J. Mass Spectrom. **345-347**, 153–159 (2013)
29. Adamson, B.D., Miller, M.E.C., Continetti, R.E.: The aerosol impact spectrometer: a versatile platform for studying the velocity dependence of nanoparticle-surface impact phenomena. EPJ Tech. Instrum. **4**(2), (2017)
30. Gamero-Castaño, M.: Induction charge detector with multiple sensing stages. Rev. Sci. Instrum. **78**, 043301 (2007)
31. Smith, J.W., Siegel, E.E., Maze, J.T., Jarrold, M.F.: Image charge detection mass spectrometry: pushing the envelope with sensitivity and accuracy. Anal. Chem. **83**, 950–956 (2011)
32. Barney, B.L., Daly, R.T., Austin, D.E.: A multi-stage image charge detector made from printed circuit boards. Rev. Sci. Instrum. **84**, 114101 (2013)
33. Elliott, A.G., Merenbloom, S.I., Chakrabarty, S., Williams, E.R.: Single particle analyzer of mass: a charge detection mass spectrometer with a multi-detector electrostatic ion trap. Int. J. Mass Spectrom. **414**, 45–55 (2017)
34. Doussineau, T., Antoine, R., Santacreu, M., Dugourd, P.: Pushing the limit of infrared multiphoton dissociation to megadalton-size DNA ions. J. Phys. Chem. Lett. **3**, 2141–2145 (2012)
35. Antoine, R., Doussineau, T., Dugourd, P., Calvo, F.: Multiphoton dissociation of macromolecular ions at the single-molecule level. Phys. Rev. A. **87**(013435), (2013)
36. Halim, M.A., Clavier, C., Dagany, X., Kerleroux, M., Dugourd, P., Dunbar, R.C., Antoine, R.: Infrared laser dissociation of single megadalton polymer ions in a gated electrostatic ion trap: the added value of statistical analysis of individual events. Phys. Chem. Chem. Phys. **20**, 11959–11966 (2018)
37. Keifer, D.Z., Shinholt, D.L., Jarrold, M.F.: Charge detection mass spectrometry with almost perfect charge accuracy. Anal. Chem. **87**, 10330–10337 (2015)
38. Pierson, E.E., Contino, N.C., Keifer, D.Z., Jarrold, M.F.: Charge detection mass spectrometry for single ions with an uncertainty in the charge measurement of 0.65 e. J. Am. Soc. Mass Spectrom. **26**, 1213–1220 (2015)
39. Keifer, D.Z., Pierson, E.E., Jarrold, M.F.: Charge detection mass spectrometry: weighing heavier things. Analyst. **142**, 1654–1671 (2017)
40. Lutomski, C.A., Lyktey, N.A., Pierson, E.E., Zhao, Z., Zlotnick, A., Jarrold, M.F.: Multiple pathways in capsid assembly. J. Am. Chem. Soc. **140**, 5784–5790 (2018)
41. Contino, N.C., Pierson, E.E., Keifer, D.Z., Jarrold, M.F.: Charge detection mass spectrometry with resolved charge states. J. Am. Soc. Mass Spectrom. **24**, 101–108 (2013)
42. Keifer, D.Z., Alexander, A.W., Jarrold, M.F.: Spontaneous mass and charge losses from single multi-megadalton ions studied by charge detection mass spectrometry. J. Am. Soc. Mass Spectrom. **28**, 498–506 (2017)
43. Elliott, A.G., Harper, C.C., Lin, H.-W., Williams, E.R.: Mass, mobility and MS^n measurements of single ions using charge detection mass spectrometry. Analyst. **142**, 2760–2769 (2017)
44. Elliott, A.G., Harper, C.C., Lin, H.-W., Susa, A.C., Xia, Z., Williams, E.R.: Simultaneous measurements of mass and collisional cross-section of single ions with charge detection mass spectrometry. Anal. Chem. **89**, 7701–7708 (2017)
45. Harper, C.C., Elliott, A.G., Lin, H.-W., Williams, E.R.: Determining energies and cross sections of individual ions using higher-order harmonics in Fourier transform charge detection mass spectrometry (FT-CDMS). J. Am. Soc. Mass Spectrom. **29**, 1861–1869 (2018)
46. Alexander, J.D., Graham, L., Calvert, C.R., Kelly, O., King, R.B., Williams, I.D., Greenwood, J.B.: Determination of absolute ion yields from a MALDI source through calibration of an image-charge detector. Meas. Sci. Technol. **21**, 045802 (2010)
47. Weinheimer, A.J.: The charge induced on a conducting cylinder by a point charge and its application to the measurement of charge on precipitation. J. Atmos. Ocean. Technol. **5**, 298–304 (1988)
48. Hogan, J.A., Jarrold, M.F.: Optimized electrostatic linear ion trap for charge detection mass spectrometry. J. Am. Soc. Mass Spectrom. (2018). https://doi.org/10.1007/s13361-018-2007-x